

# Multiwalled carbon nanotubes intratracheally instilled into the rat lung induce development of pleural malignant mesothelioma and lung tumors

Masumi Suzui,<sup>1</sup> Mitsuru Futakuchi,<sup>1</sup> Katsumi Fukamachi,<sup>1</sup> Takamasa Numano,<sup>1</sup> Mohamed Abdelgied,<sup>2,3,4</sup> Satoru Takahashi,<sup>2</sup> Makoto Ohnishi,<sup>5</sup> Toyonori Omori,<sup>6</sup> Shuji Tsuruoka,<sup>7</sup> Akihiko Hirose,<sup>8</sup> Jun Kanno,<sup>9</sup> Yoshimitsu Sakamoto,<sup>10</sup> David B. Alexander,<sup>3</sup> William T. Alexander,<sup>3</sup> Xu Jiegou<sup>3,11</sup> and Hiroyuki Tsuda<sup>3</sup>

<sup>1</sup>Department of Molecular Toxicology, Nagoya City University Graduate School of Medical Sciences, Nagoya; <sup>2</sup>Department of Experimental Pathology and Tumor Biology, Nagoya City University Graduate School of Medical Sciences, Nagoya; <sup>3</sup>Nanotoxicology Project, Nagoya City University, Nagoya, Japan; <sup>4</sup>Forensic Medicine and Toxicology, Faculty of Veterinary Medicine, Beni-Suef University, Beni-Suef, Egypt; <sup>5</sup>Japan Industrial Safety and Health Association, Japan Bioassay Research Center, Kanagawa; <sup>6</sup>National Center for Child Health and Development, Tokyo; <sup>7</sup>Institute of Carbon Science and Technology, Shinshu University, Nagano City; <sup>8</sup>Division of Risk Assessment, National Institute of Health Sciences, Akihiko Hirose, Tokyo; <sup>9</sup>Division of Cellular and Molecular Toxicology, National Institute of Health Sciences, Tokyo; <sup>10</sup>Department of Pharmaceutical and Environmental Sciences, Tokyo Metropolitan Institute of Public Health, Tokyo, Japan; <sup>11</sup>Department of Immunology, College of Basic Medical Sciences, Anhui Medical University, Hefei, China

## Key words

Intratracheal instillation, lung tumors, malignant mesothelioma, multiwalled carbon nanotubes, rat

## Correspondence

Xu Jiegou, Department of Immunology, College of Basic Medical Sciences, Anhui Medical University, Meishan Road 81, Hefei 230032, China.

Tel: +86-551-6516-1139; Fax: +86-551-6516-1139;

E-mail: xujiegou@ahmu.edu.cn

and

Hiroyuki Tsuda, Nanotoxicology Project, Nagoya City University, 3-1 Tanabe-Dohri, Mizuho-ku, Nagoya 466-8603, Japan. Tel: +81-052-836-3496; Fax: +81-052-836-3497;

E-mail: htsuda@phar.nagoya-cu.ac.jp

## Funding Information

Princess Takamatsu Cancer Research Fund, (Grant/Award Number: 'H24') Health and Labor Sciences Research Grants of Japan, (Grant/Award Number: 'H21-kagaku-ippan-008', 'H22-kagaku-ippan-005', 'H24-kagaku-sitei-009', 'H25-kagaku-ippan-004').

Received March 14, 2016; Revised April 17, 2016;

Accepted April 19, 2016

*Cancer Sci* 107 (2016) 924–935

doi: 10.1111/cas.12954

Carbon nanotubes have a fibrous structure and physical properties similar to asbestos.<sup>(1)</sup> Unlike spherical particles and short fibers, long fibers cannot effectively pass from the pleural cavity into the lymphatic system through pores in the chest wall, resulting in deposition in the pleural cavity.<sup>(1)</sup> The high concentrations of asbestos fibers, especially long thin chrysotile fibers, that were found in the parietal pleura in patients with plaques and malignant mesotheliomas by Kohyama and Suzuki can be attributed to this fact.<sup>(2)</sup> The similarity between multiwalled carbon nanotubes (MWCNT) and asbestos raises concern that the widespread use of MWCNT may cause an asbestos-like pandemic of disease.<sup>(1,3)</sup>

Recent studies have shown that direct injection of MWCNT-7 into the peritoneal cavity or the scrotum induced malignant

Multiwalled carbon nanotubes (MWCNT) have a fibrous structure and physical properties similar to asbestos and have been shown to induce malignant mesothelioma of the peritoneum after injection into the scrotum or peritoneal cavity in rats and mice. For human cancer risk assessment, however, data after administration of MWCNT via the airway, the exposure route that is most relevant to humans, is required. The present study was undertaken to investigate the carcinogenicity of MWCNT-N (NIKKISO) after administration to the rat lung. MWCNT-N was fractionated by passing it through a sieve with a pore size of 25  $\mu\text{m}$ . The average lengths of the MWCNT were 4.2  $\mu\text{m}$  before filtration and 2.6  $\mu\text{m}$  in the flow-through fraction; the length of the retained MWCNT could not be determined. For the present study, 10-week-old F344/Crj male rats were divided into five groups: no treatment, vehicle control, MWCNT-N before filtration, MWCNT-N flow-through and MWCNT-N retained groups. Administration was by the trans-tracheal intrapulmonary spraying (TIPS) method. Rats were administered a total of 1 mg/rat during the initial 2 weeks of the experiment and then observed up to 109 weeks. The incidences of malignant mesothelioma and lung tumors (bronchiolo-alveolar adenomas and carcinomas) were 6/38 and 14/38, respectively, in the three groups administered MWCNT and 0/28 and 0/28, respectively, in the control groups. All malignant mesotheliomas were localized in the pericardial pleural cavity. The sieve fractions did not have a significant effect on tumor incidence. In conclusion, administration of MWCNT to the lung in the rat induces malignant mesothelioma and lung tumors.

mesotheliomas in rats and mice.<sup>(4–7)</sup> While these administration routes are not directly applicable to human risk assessment, as the exposure route in humans is by inhalation,<sup>(3,8)</sup> other recent studies have demonstrated that MWCNT administered to the lung translocates into the pleural cavity in mice and rats.<sup>(9–16)</sup> Taken together, these studies illustrate that, like asbestos, MWCNT is able to induce cancer of the mesothelium and, when administered to the lung, is able to be translocated from the lung into the pleural cavity.

Our studies have directly demonstrated that in rats MWCNT administered to the lung by the trans-tracheal intrapulmonary spraying (TIPS) method, an apposite antecedent to costly aerosol inhalation studies, translocated to the pleural cavity and caused marked inflammatory reactions, accumulations of

macrophages phagocytosing the MWCNT fibers, and hyperplastic proliferation of the visceral mesothelium.<sup>(11,16)</sup> Importantly, pleural translocation and induction of lesions in the lung and pleura by MWCNT administered to the lung was size and shape dependent.<sup>(16)</sup> Based on these findings, we conducted the present study to investigate the possibility that MWCNT-N administered to the lung is carcinogenic to the pleura and lung. We also fractionated the MWCNT-N by passing it through a sieve with a pore size of 25  $\mu\text{m}$  to investigate whether there were any size-dependent effects on induction of chronic inflammation or carcinogenesis associated with different fiber lengths.

## Materials and Methods

**Preparation of the multiwalled carbon nanotube fractions.** The MWCNT-N, provided by NIKKISO, Tokyo, Japan, with an original (at the production site) size of 3.5  $\mu\text{m}$  in length and 1–20 nm in diameter, was suspended in saline containing 0.5% Pluronic F68 (PF68) (Sigma-Aldrich, St. Louis, MO, USA), which prevents aggregation of MWCNT,<sup>(17)</sup> to a final concentration of 250  $\mu\text{g}/\text{mL}$ . We found that this formula has the best dispersing performance without having toxic effects in the lung (Jiegou Xu, unpublished data). After adding MWCNT-N into this dispersant, the mixture was homogenized for 1 min four times at 3000 rpm in a Polytron PT1600E benchtop homogenizer (Kinematika, Littau, Switzerland). Then, 50 mL of the MWCNT-N suspension was fractionated by passing it through a sieve with a pore size of 25  $\mu\text{m}$ . The flow-through fraction was centrifuged at 10 000  $g$  for 30 min and the upper 40 mL of the supernatant was removed. The MWCNT was homogenized and the concentration of the MWCNT was determined by optical density.<sup>(18)</sup> The MWCNT was brought to a final concentration of 250  $\mu\text{g}/\text{mL}$  in 0.5% PF68. The retained fraction was resuspended in 20 mL 0.5% PF68, the concentration determined, and the suspension was brought to a final concentration of 250  $\mu\text{g}/\text{mL}$  in 0.5% PF68. Photographs of the three preparations (unfiltered, the flow-through fraction and the retained fraction) were obtained using a scanning microscope (SEM) (Model S-4700 Field Emission SEM; Hitachi High Technologies, Tokyo, Japan) at 5–10 kV, and the lengths of MWCNT-N fibers were measured using a digital map meter (Comcurve-9 Junior; Koizumi Sokki, Niigata, Japan); at least 500 fibers in three to five SEM photos of the unfiltered and flow-through fractions were measured. The length of the unfiltered MWCNT-N fibers was  $4.2 \pm 2.9 \mu\text{m}$  and the length of the MWCNT in the flow-through fraction was  $2.6 \pm 1.6 \mu\text{m}$ . The lengths of the MWCNT-N fibers in the retained fraction could not be measured because of the formation of dense agglomerates due to the loss of the PF68 dispersant solution. The diameter of the MWCNT-N fibers was mostly (93.4%) within 30–80 nm. The iron content was 0.046% by weight (Ogata, Tokyo Metropolitan Institute of Public Health, unpublished data).

**Animals and treatment.** One hundred 10-week-old F344/Crj male rats (Charles River Laboratories Japan, Yokohama, Japan) were divided into five groups of 20 animals each: Group 1, no treatment; Group 2, vehicle; Group 3, unfiltered MWCNT-N; Group 4, MWCNT-N flow-through fraction; Group 5, MWCNT-N retained fraction. The MWCNT suspensions were sonicated for 30 min shortly before use to minimize aggregation. Each preparation was administered to the rats by the trans-tracheal intrapulmonary spraying (TIPS) method, an apposite antecedent to costly aerosol inhalation studies, at a dose of 125  $\mu\text{g}$  in 0.5 mL vehicle per rat. The animals were

administered MWCNT-N eight times (total 1 mg/rat) over a 2-week period. Briefly, rats were anaesthetized by inhalation of 5% isoflurane; the mouth was fully opened with the tongue gently held and the nozzle of a microsyringe (series IA-1B Intratracheal Aerosolizer; Penn-century, Philadelphia, PA, USA) connected to a 1-mL syringe was inserted through the larynx into the trachea; the 0.5-mL suspension was sprayed into the lungs synchronizing with spontaneous respiratory inhalation.<sup>(11,16,19–21)</sup>

In preliminary studies, we confirmed that the dosed materials, particles and fibers reached most of the terminal alveoli without causing obvious respiratory distress. The initial number of animals was 20 rats in each group. At the end of week 2, 5 rats from each group were killed 24 h after the last administration of MWCNT and used to measure the dosed amount of MWCNT-N. The remaining 15 rats were observed until the end of the experiment at week 109. Moribund animals were killed by exsanguination from the inferior vena cava under the deep anesthesia induced by 10% isoflurane. Rats that survived for at least 63 weeks (the first death caused by tumor development occurred at week 64) were included in the analysis of the experimental data. The major organs, the lung, pleural wall, peritoneal wall, brain, liver, kidney, spleen and mediastinal, submandibular and mesentery lymph nodes, were excised, fixed in ice-cold 4% paraformaldehyde and processed for histological examination. The study was conducted according to the Guidelines for the Care and Use of Laboratory Animals of Nagoya City University Medical School (Nagoya, Japan). Histopathological evaluation was peer reviewed by Dr Shoji Fukusima, Director, Japan Bioassay Research Center, and Dr Tomoyuki Shirai, Emeritus Professor, Department of Experimental Pathology and Tumor Biology, Nagoya City University Graduate School of Medical Sciences. Dr Tsuda (the corresponding author), Dr Fukushima and Dr Shirai are Board Pathologists of the Japan Society of Toxicologic Pathology (Diplomate of JSTP) and the Japan Society of Pathology.

**Immunohistochemistry.** Briefly, tissue sections were deparaffinized with xylene, hydrated through a graded ethanol series and water, incubated in heat processor solution pH6 (715281; Nichirei Biosciences, Tokyo, Japan) at 100°C for 40 min., incubated in 3%  $\text{H}_2\text{O}_2$  (715242 Nichirei Biosciences, Tokyo, Japan) for 15 min, blocked with 5% BSA 5% serum in PBS for 1 h at room temperature, incubated overnight with 1° Ab at 4°C, incubated with 2° Ab (414191, Nichirei Biosciences, Tokyo, Japan) for 1 h at room temperature, visualized with DAB (425011 Nichirei Biosciences, Tokyo, Japan), and counterstained with hematoxylin. Primary antibodies used were calretinin (bs-0062R Bioss Antibodies, Boston MA, USA) diluted 1:100, podoplanin (11-035; AngioBio, San Diego CA, USA) diluted 1:20, thyroid transcription factor-1 (sc-13040; Santa Cruz Biotechnology, Dallas TX, USA) diluted 1:50, and Wilms tumor protein (sc-192, Santa Cruz Biotechnology) diluted 1:50. Because in rats, as in humans, ERC/mesothelin is not a good marker to differentiate epithelial carcinomas from sarcomatous mesotheliomas, staining with ERC/mesothelin was not performed.

**Observation of multiwalled carbon nanotubes in the lung by polarized light microscopy and scanning electron microscopy.** The MWCNT fibers in H&E stained slides of lung tissue and chest wall sections were observed with polarized light microscopy (BX51N-31P-O; Olympus, Tokyo, Japan) at 400 $\times$  magnification. The exact localization of the illuminated fibers was confirmed in the same H&E-stained sections after removing the polarizing filter. For SEM, H&E stained slides were immersed in xylene for 2–3 days to remove the cover glass,

immersed in 100% ethanol for 10 min to remove the xylene, and air-dried for 2 h at room temperature. The slides were then coated with platinum for viewing the MWCNT fibers by SEM (Model S-4700 Field Emission Scanning Electronic Microscope, Hitachi High Technologies) at 5–10 kV.

**Measurement of multiwalled carbon nanotubes in the lung.** This procedure is based on a previously published report.<sup>(22)</sup>

**Sample preparation.** Paraformaldehyde fixed lung samples were allowed to react with Clean 99-K200<sup>R</sup> (C99) (Clean Chemical, Osaka, Japan) at room temperature overnight. The solution was then centrifuged at  $13\,000 \times g$  for 10 min and the supernatant was removed. The precipitate was resuspended in 1 mL of 9.6% PBS containing 0.1% Tween 80 (TW-solution) followed by a second centrifugation at  $13\,000 \times g$  for 10 min. The pellet was resuspended in 100- $\mu$ L concentrated sulfuric acid to remove the organic content. 1-mL TW-solution was stirred into the acid-MWCNT-N mixture. 25  $\mu$ L of a solution of 0.125  $\mu$ g/mL Benzo[ghi]perylene (B[ghi]P) in acetonitrile was then added, and the B[ghi]P was allowed to adsorb onto the MWCNT for 15 min. The mixture was passed through a Nuclepore membrane filter (Whatman 111109, pore size 0.8  $\mu$ m, diameter 47 mm; Fisher Scientific, Waltham MA, USA), and the MWCNT containing region was punched out and placed in 1-mL acetonitrile and sonicated for 10 s with an ultrasonic homogenizer (VP-30S, 20 kHz, 300 W; TAITEC, Tokyo, Japan). The solution was then filtered for HPLC analysis of the extracted B[ghi]P.

**Generation of a calibration curve.** A 10-mg sample of MWCNT-N was added to 40 mL of the TW-mixture and sonicated for 30 min. The solution was diluted to 2  $\mu$ g/mL with C99. This solution was used to prepare additional standards of 0.4, 0.8, 1.2 and 1.6  $\mu$ g/mL MWCNT-N in C99. Then 0.1 mL of each of the standards was centrifuged ( $13\,000 \times g$ , 10 min) and the pellets resuspended in concentrated sulfuric acid and treated as described above.

**Statistical analyses.** Tumor incidence was analyzed using Fisher's exact test, with significance set at  $P \leq 0.05$ .

## Results

**Effect of sieve fractionation on the size of multiwalled carbon nanotubes.** The MWCNT-N from NIKKISO (original reported size of 3.5  $\mu$ m in length and 1–20 nm in diameter) was suspended in 20-mL saline containing 0.5% Pluronic F68 (PF68) to a final concentration of 250  $\mu$ g/mL for administration to rats. A portion of the MWCNT-N was fractionated by passing it through a sieve with a pore size of 25  $\mu$ m to obtain fractions with different length MWCNT. The length of the unfiltered fibers and the fibers in the flow-through fraction in the administration dispersant showed a normal distribution in the range of <1–10  $\mu$ m. The mean lengths of the unfiltered MWCNT-N and MWCNT-N in the flow-through fraction were  $4.2 \pm 2.9$  and  $2.6 \pm 1.6$   $\mu$ m, respectively. The size of the retained MWCNT-N could not be measured because of the dense agglomerates the retained fibers formed due to loss of the PF68 dispersant during fractionation. SEM images of the three fractions are shown in Figure 1. For the rats administered unfiltered MWCNT-N, the size of the fibers in the lung tissue slides tended to be smaller than in the administered preparation (Table 1).

**Amount of multiwalled carbon nanotubes in the lung.** Rats were divided into five groups: no treatment, vehicle control, unfiltered MWCNT-N, MWCNT-N flow-through and MWCNT-N retained groups. MWCNT was administered to the

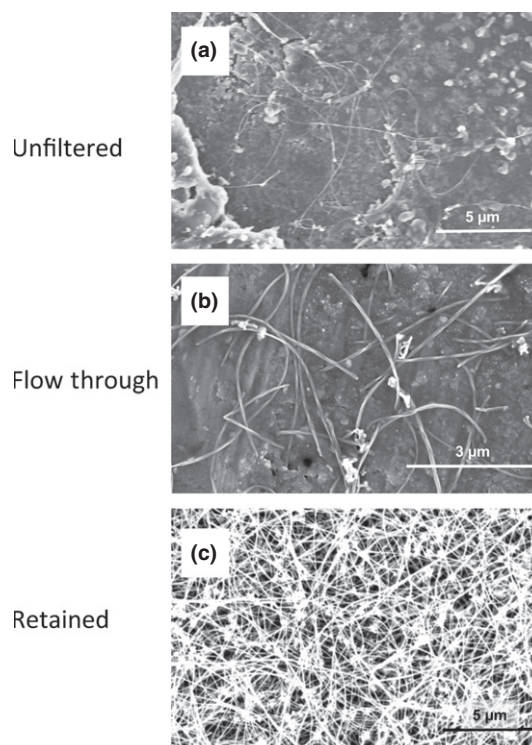


**Fig. 1.** Before administration, a portion of the multiwalled carbon nanotube (MWCNT) suspension was fractionated by passing it through a sieve with a pore size of 25  $\mu$ m. Scanning microscope images of MWCNT-N in the (a) unfiltered preparation, (b) flow-through fraction and (c) retained fraction are shown. The mean length of the unfiltered MWCNT-N in the administration dispersant was  $4.2 \pm 2.9$   $\mu$ m and that of the MWCNT-N in the flow-through fraction was  $2.6 \pm 1.6$   $\mu$ m. The size of the MWCNT-N retained by the filtering sieve could not be measured because of the dense agglomerates the retained fibers formed due to the loss of the PF68 dispersant during fractionation.

**Table 1.** Size of MWCNT-N in the preparation medium and in the lung tissue

MWCNT-N fraction	MWCNT-N in the preparation medium before administration	MWCNT-N in the lung tissue	
		Alveolar wall	Tumor area
Unfiltered	$4.2 \pm 2.9$ †	$3.1 \pm 1.0$	$2.0 \pm 0.4$
Flow-through	$2.6 \pm 1.6$	$2.8 \pm 0.9$	$2.6 \pm 0.6$
Retained	>2.6	$3.2 \pm 0.8$	$3.2 \pm 0.7$

†Mean  $\pm$  SD  $\mu$ m. MWCNT, multiwalled carbon nanotubes.

lung by the TIPS method eight times over a 2-week period; 24 h after the last treatment, 5 rats from each group were killed and the amount of MWCNT in their lungs was determined (Table 2). At the end of the experiment, week 109, the MWCNT remaining in the lungs of rats administered unfiltered MWCNT-N and the flow-through and retained MWCNT fractions were 25.4, 48.0 and 26.3%, respectively, of the amount measured at week 2 (Table 2).

**Localization of multiwalled carbon nanotubes.** Figure 2 shows MWCNT-N in the lung and lymph node. MWCNT-N was mostly found in the lung alveoli and had a needle-like or granular appearance. MWCNT-N fibers were also present in the mediastinal space, as evidenced by their presence in mediastinal lymphnodes and periaortic connective tissue. In the alveoli,

**Table 2.** Amount of MWCNT-N in the lung at weeks 2 and 109

Rats†	Week 2		Rats†	Week 109		Ratio of week 109 to week 2 (%)
	MWCNT-N Fraction	Amount‡		MWCNT-N Fraction	Amount‡	
5	Unfiltered	1912 ± 162	5	Unfiltered	486 ± 44	25.4
4	Flow-through	887 ± 131	4	Flow-through	426 ± 116	48.0
5	Retained	1019 ± 165	5	Retained	268 ± 43	26.3

†Number of rats examined. ‡ $\mu\text{g}$  MWCNT-N per gram wet-weight paraformaldehyde fixed lung tissue. MWCNT, multiwalled carbon nanotubes.

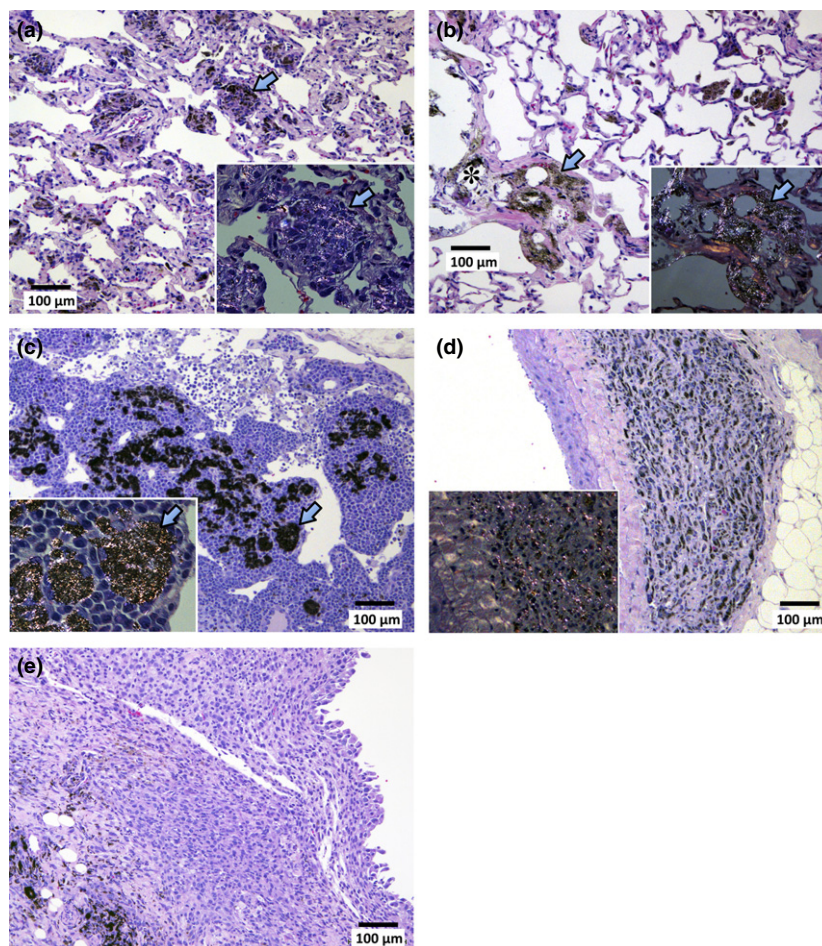


**Fig. 2.** Accumulation of multiwalled carbon nanotubes (MWCNT) in the lung (a,b) and lymph node (c,d). MWCNT-N was found in the lung alveoli either in the granulation tissue or macrophages. (a) MWCNT-N shows granular and needle like shapes. Aggregations of MWCNT-phagocytosed macrophages can be seen (arrow). The inset shows a polarizing lens image of the aggregation of MWCNT-phagocytosed macrophages; arrows point to the same macrophage aggregation in the main panel and the inset. MWCNT-N aggregates that cause polarization can clearly be seen in the inset. Granular agglomerations of MWCNT-N do not cause polarization. (b) MWCNT-N also caused thick fibrotic granulation tissue formation (arrow) and calcification (\*). The inset shows a polarizing lens image of granulation tissue with deposition of MWCNT-N. Arrows point to the same lesion in the main panel and the inset. (c) Accumulation of MWCNT-N in the mediastinal lymph node. The inset shows a polarizing lens image. Arrows point to the same MWCNT-N accumulations in the main panel and the inset. (d) Accumulation of MWCNT-N in periaortic connective tissue showing fibrotic thickening. The inset shows a polarizing lens image. (e) MWCNT-N is present in the periphery of the malignant mesothelioma tissue.

MWCNT was found in macrophages (Fig. 2a) and in granulation tissue (Fig. 2b). Abundant MWCNT-N was also found in bronchial and mediastinal lymph nodes (Fig. 2c), and periaortic connective tissue (Fig. 2d). Needle-shaped MWCNT aggregates detected by polarized light microscopy can be seen in Figure 2(a and b). Damage of the submucosal tissue of the tracheal wall through accumulation of large agglomerates of MWCNT (Fig. 2c) and fibrotic thickening of periaortic connective tissue (Fig. 2d) were also noted; thickening of pleural tissue was not observed in untreated or vehicle control animals.

**Results of the 109-week study.** All moribund animals were killed by exsanguination from the inferior vena cava under deep anesthesia and autopsied. Prior to the first death due to cancer-related causes, six animals died. These animals were excluded from the study. At week 64 an animal died from lung tumors. Therefore, all animals surviving for 63 weeks or

more were included in the study. Figure 3 shows a Kaplan-Meier survival plot. There are no differences in survival times between any of the groups and the vehicle control group.

Mesothelioma-bearing animals tended to die before week 109: in the unfiltered group, 1 mesothelioma-bearing rat died during week 96, a second during week 101, and a third during week 108; in the flow-through group, 1 mesothelioma-bearing rat died during week 79 and a second during week 99. The third mesothelioma-bearing rat in the flow-through group survived until the end of the experiment (week 109); this rat also had a lung adenocarcinoma.

In contrast to the mesothelioma-bearing rats, seven rats bearing lung tumors died before week 109 and six rats bearing lung tumors survived until the end of the experiment: in the unfiltered group, 1 rat bearing a lung adenoma died during week 74 and 1 bearing a lung adenocarcinoma during week 108. The 2 other lung adenocarcinoma-bearing bearing rats in

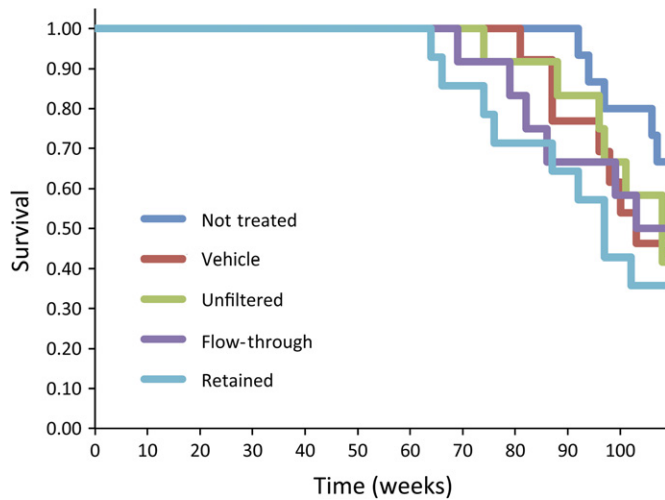


**Fig. 3.** Kaplan–Meier survival plot of the rats in the untreated, vehicle control, unfiltered multiwalled carbon nanotubes (MWCNT), flow-through MWCNT fraction, and retained MWCNT fraction groups.

this group survived until the end of the experiment. In the flow-through group, 1 rat bearing a lung adenoma died during week 82 and 1 bearing a lung adenocarcinoma died during week 103. The second rat bearing a lung adenocarcinoma survived until the end of the experiment; this rat also had a mesothelioma. In the retained group, 1 rat bearing a lung adenoma died during week 74 and a second during week 76, and 1 rat bearing a lung adenocarcinoma died during week 64 and a second during week 87. The 3 other lung adenocarcinoma-bearing rats in this group survived until the end of the experiment.

The incidence of malignant mesothelioma in the three MWCNT groups combined, 6/38 (15.8%), was significantly higher compared to the two control groups combined, 0/28 (0%;  $P = 0.034$ ) (Table 3). While no statistically significant differences in the incidence of malignant mesotheliomas were found among the three groups administered the different MWCNT fractions, it is noteworthy that the groups administered the unfiltered and flow-through fractions had incidences of 3 mesothelioma cases each and the group administered the retained fraction did not have any cases of mesothelioma.

MWCNT fraction	Rats	Malignant mesothelioma Pericardial and/or pleura (%)	Lung tumors			Total tumor burden (%)
			Adenoma	Adenocarcinoma	Combined (%)	
NT	15	0 (0.0)	0	0	0 (0.0)	0 (0.0)
V	13	0 (0.0)	0	0	0 (0.0)	0 (0.0)
NT + V	28	0 (0.0)	0	0	0 (0.0)	0 (0.0)
U	12	3† (25.0)	1	3†	4 (33.3)	7 (58.3)
FT	12	3 (25.0)	1	2	3 (25.0)	6 (50.0)
R	14	0 (0.0)	2	5	7 (50.0)	7 (50.0)
U + FT + R	38	6 (15.8)*	4	10	14 (36.8)**	20 (52.6)**

\* $P < 0.05$ ; \*\* $P < 0.001$  versus the control groups (NT + V). †One rat had both a malignant mesothelioma and a lung adenocarcinoma. FT, flow-through; MWCNT, multiwalled carbon nanotubes; NT, no treatment; R, retained; U, unfiltered; V, vehicle. Average length: U =  $4.2 \pm 2.9 \mu\text{m}$ ; FT =  $2.6 \pm 1.6 \mu\text{m}$ ; R was not measurable.

**Table 3.** Incidence of pleural malignant mesothelioma and lung tumors

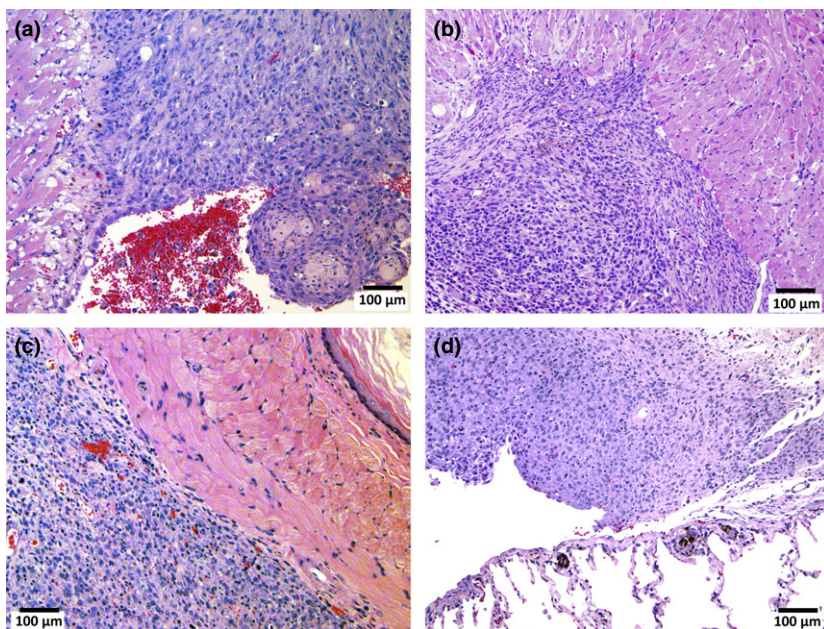


**Fig. 4.** Malignant mesotheliomas in the pleural/mediastinal cavity. Malignant mesothelioma showing invasion of the pericardium (a), myocardium (b), periesophageal tissue (c) and visceral pleura (d).

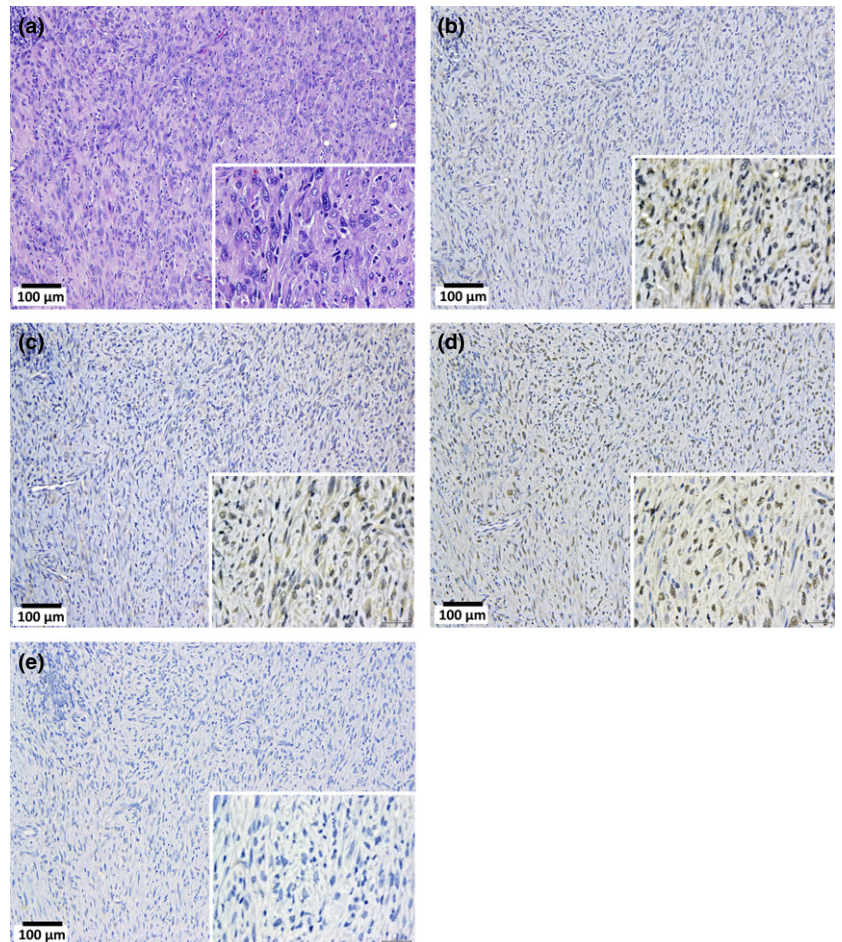


**Fig. 5.** Malignant mesothelioma, sarcomatoid type, in the pleural cavity. (a) Tumor cells arranged in a solid manner. Immunostaining of calretinin (b), Wilms tumor protein (WT-1) (c), podoplanin (Pod) (d), and thyroid transcription factor-1 (TTF-1) (e). In the high power magnification images (inset), the cytoplasm of the tumor cells were faintly stained by calretinin and Wilms tumor protein. Nuclei are also faintly stained by Pod. Cytoplasm and nuclei are entirely unstained by TTF-1.

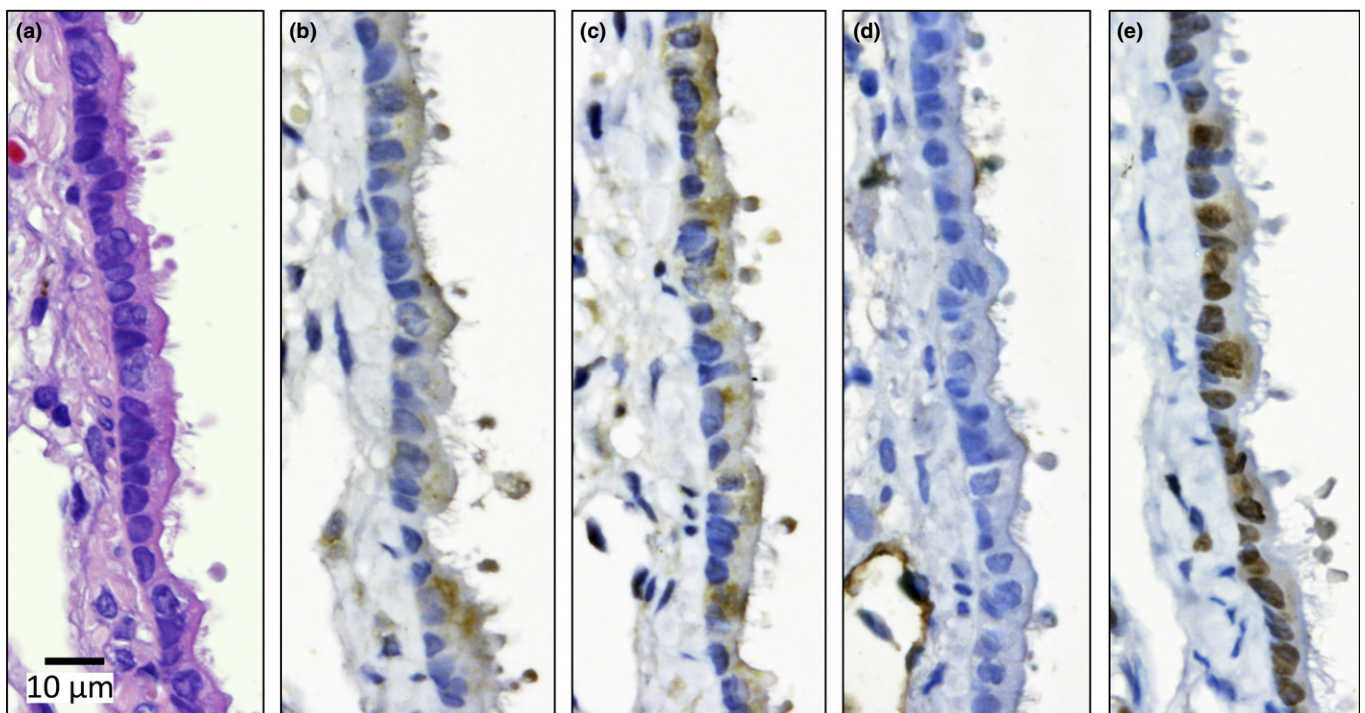


**Fig. 6.** Bronchiolar epithelium of 109 week old untreated rat. H&E (a) and calretinin (Cal) (b), Wilms tumor protein (WT-1) (c), podoplanin (d) and thyroid transcription factor-1 (TTF-1) (e) staining. The cytoplasm is slightly stained by Cal and WT-1. Nuclei are clearly positive for TTF-1.

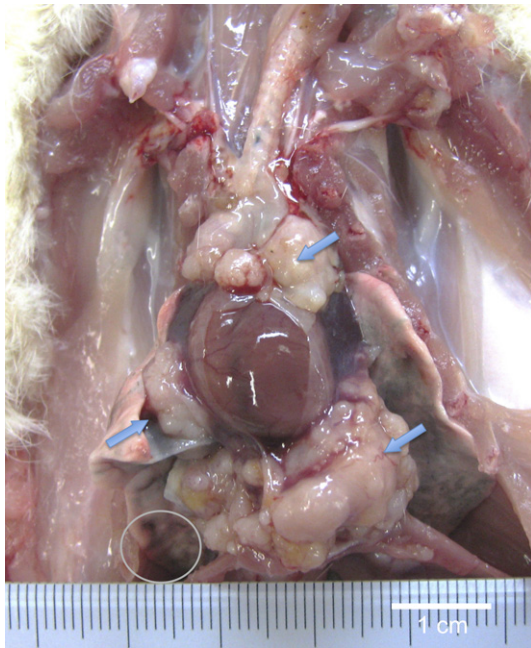
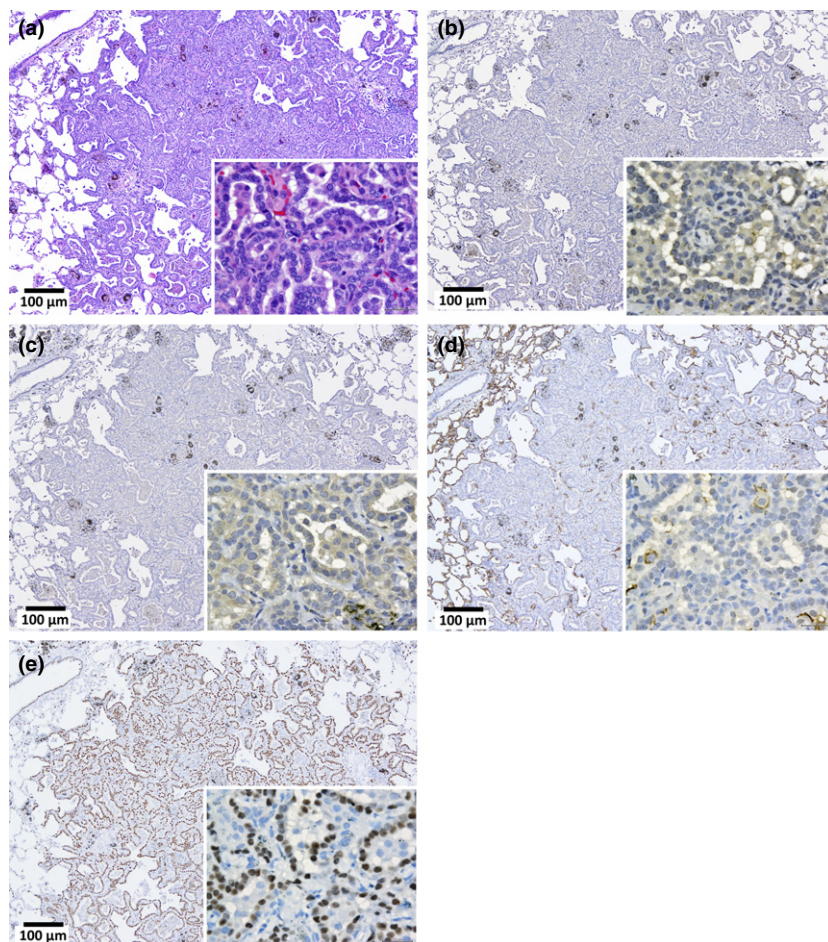


**Fig. 7.** Gross appearance of lung adenocarcinoma in the pericardial pleural cavity. Histologically, the tumor is composed of packed small epithelial-like cells forming incomplete glandular structures (see Figure 11a) with invasion of pericardial and diaphragm tissues (arrows). The tumor was positive for TTF-1. Small tumor nodules of the same histological appearance were found in the lung (circle).

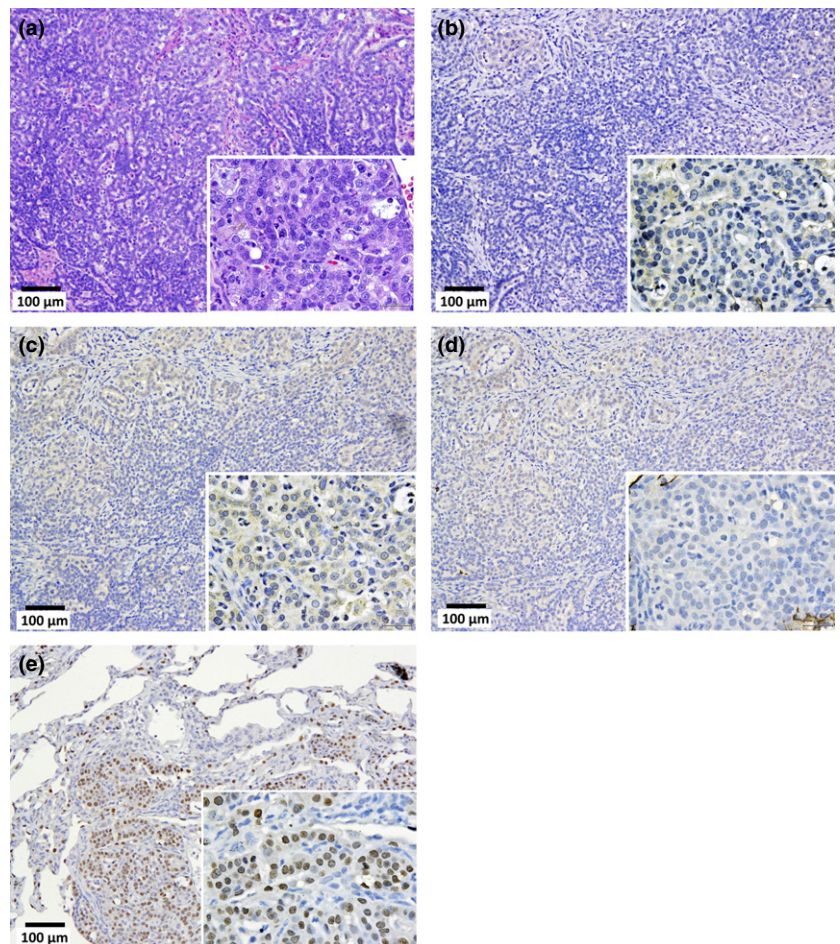
Mesotheliomas were irregularly shaped whitish masses with diameters of up to 1.5 cm. All the malignant mesotheliomas were localized in the mediastinal space (*Cavum mediastinale*), showing adhesion to the lung and heart or invasion of the lung parenchyma, peri-cardium and myo-cardium (Fig. 4). The primary site of these mesotheliomas could not be determined because all the tumor masses were at an advanced stage. None of the mesotheliomas were located in the lateral parietal pleura. One case of mesothelioma in the unfiltered group (“U” in Table 3) showed invasion of the mesothelioma into the lung. Interestingly, this tumor also showed invasion into the lung adenocarcinoma present in this animal. The mesotheliomas originated from mesothelial tissue outside of the lung and, consequently, were negative for thyroid transcription factor-1 (TTF-1) (Fig. 5). Figure 6 shows that TTF-1 clearly stains normal bronchiolar epithelium.

Figure 7 is a macroscopic view of a lung adenocarcinoma. Lung tumors, both adenomas and adenocarcinomas, were positive for TTF-1 (Figures 8–11). The incidence of lung tumors (bronchiolo-alveolar adenoma and carcinoma) (14/38; 36.8%) was significantly higher than the control group (0/28; 0%) ( $P < 0.001$ ) (Table 3). No obvious site prevalence was noted in the lung tumors. No significant difference in the incidence of lung tumors or total tumor burden was found among the three groups administered the different MWCNT-N sieve fractions.

The Incidences of tumors in other organs did not show any statistical difference from the controls (Table 4). Two cases of



**Fig. 8.** Lung bronchiolo-alveolar adenoma (adenoma). H&E (a), calretinin (Cal) (b), Wilms tumor protein (WT-1) (c), podoplanin (d) and thyroid transcription factor-1 (TTF-1) (e) staining. The cytoplasm is slightly stained by Cal and WT-1. Nuclei are clearly positive for TTF-1.



**Fig. 9.** Bronchiolo-alveolar carcinoma (adenocarcinoma) of the lung. H&E (a), calretinin (Cal) (b), Wilms tumor protein (c), podoplanin (d) and thyroid transcription factor-1 (TTF-1) (e) staining. The cytoplasm is slightly stained by Cal and Wilms tumor protein (WT-1). Nuclei are clearly positive for TTF-1.

well-differentiated mesothelioma in the peritoneal cavity showing continuation to the tunica vaginalis were found in the vehicle control group and one each in the flow-through and retained MWCNT fraction administered groups. These peritoneal mesotheliomas were excluded from the statistical analysis of pleural mesotheliomas because of probable scrotal tissue origin.<sup>(23)</sup>

## Discussion

Based on the fibrous structure and physical properties of MWCNT, there is concern that without proper controls, use of this material could lead to an asbestos-like pandemic of disease.<sup>(3)</sup> Initial studies showed that after administration of MWCNT by inhalation and tracheal instillation, MWCNT reached the pleura and caused toxicity to both the lung and pleura.<sup>(9,10,13–15,17,24–27)</sup> In addition, other studies showed that administration of MWCNT-7 by intraperitoneal or intrascrotal injection caused mesotheliomas in male *p53*<sup>+/-</sup> mice and rats.<sup>(4–7)</sup> Thus, like asbestos, MWCNT is able to induce cancer of the mesothelium and, when administered to the lung, is toxic to both the lung and pleura. While these studies did not directly show that MWCNT administered via the airway, the exposure route most relevant to humans, was carcinogenic, they did demonstrate the possibility that inhaled MWCNT may be carcinogenic. A recent study, however, did demonstrate that inhalation of MWCNT-7 promoted lung tumors initiated by methylcholanthrene in mice, directly demonstrating the carcinogenic potential of inhaled

MWCNT.<sup>(28)</sup> Based on the above findings, MWCNT-7 was evaluated as a Group 2B carcinogen, sufficient evidence of carcinogenicity in animals and possibly carcinogenic to humans, by WHO/International Agency for Research on Cancer (WHO/IARC).

The primary objective of the present study was to determine whether administration of MWCNT-N via the airway to the rat lung using the TIPS method, an apposite antecedent to costly aerosol inhalation studies, was carcinogenic to the lung or pleural tissues. Our earlier studies were the first reports that MWCNT administered to the lung induced inflammation and hyperplastic proliferative lesions of the mesothelium.<sup>(11,16)</sup> The work reported in the present study is the first report to demonstrate that inhaled MWCNT is carcinogenic to the pleura, clearly indicating that MWCNT administered to the lung has the potential to induce malignant mesothelioma. In addition, the present study demonstrates that instillation of MWCNT into the lung induces lung tumors. Thus, exposure of rats to MWCNT via the airway results in malignant mesothelioma and lung tumors, extending the IARC classification of MWCNT-7 as a group 2B carcinogen to other species of MWCNT; Table 5 compares MWCNT-7 and MWCNT-N.<sup>(4,5)</sup>

The incidences of tumors in other organs did not show any statistical difference from the controls (Table 4), including the peritoneal cavity mesotheliomas in the vehicle control group (2 mesotheliomas), the flow-through group (1 mesothelioma) and the retained MWCNT fraction group (1 mesothelioma). These peritoneal mesotheliomas were excluded from the statistical analysis of pleural mesotheliomas because aged male

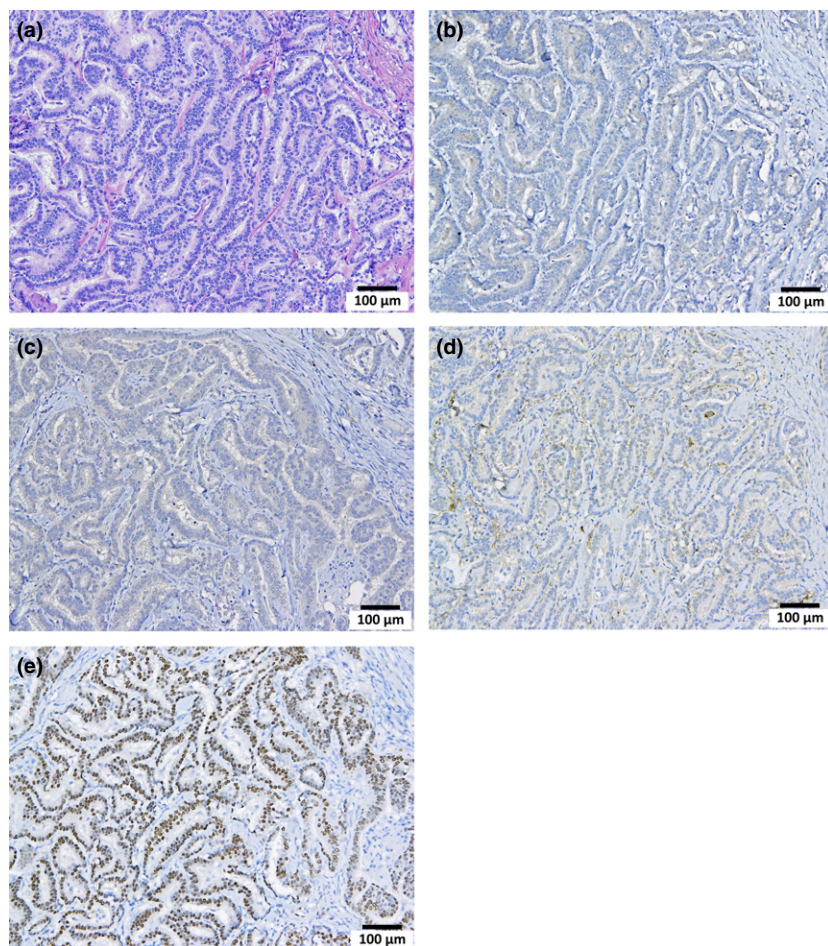


**Fig. 10.** Adenocarcinoma of the lung forming a large mass in the pleural cavity with invasion of the heart and diaphragm and remote metastasis to the kidney. H&E (a), calretinin (Cal) (b), Wilms tumor protein (c), podoplanin (d) and thyroid transcription factor-1 (TTF-1) (e) staining. The cytoplasm is slightly stained by Cal and Wilms tumor protein. Nuclei are clearly positive for TTF-1.

Fischer 344/N rats are prone to developing spontaneous peritoneal mesotheliomas that arise predominantly from the tunica vaginalis of the testes.<sup>(23)</sup>

In the present study, rats were exposed to 1 mg of MWCNT-N per animal. Because the alveolar surface area of the rat lung (both lungs) is  $0.4 \text{ m}^2$ ,<sup>(29)</sup> this dose is approximately  $2.5 \text{ mg/m}^2$  alveolar surface area. This is approximately fourfold higher than that used in the MWCNT-7 inhalation study by Sargent *et al.*<sup>(28)</sup> Mice were exposed to  $5 \text{ mg/m}^3$  MWCNT-7 for 5 h/day for 15 days using a whole body inhalation system resulting in a lung burden of  $31.2 \text{ µg}$  MWCNT/mouse. Because the alveolar surface area of the mouse is approximately  $0.05 \text{ m}^2$ , the mice were exposed to  $624 \text{ µg}$  MWCNT per  $\text{m}^2$  alveolar surface area. For a human exposed to MWCNT in the workplace, assuming a minute ventilation of  $20 \text{ L/min}$  for a person doing light work,<sup>(30)</sup> 8 h exposure per day, and a workload of 48 weeks for 45 years, a worker exposed to  $1 \text{ µg/m}^3$  would inhale approximately  $104 \text{ mg}$  MWCNT over their working life. Because the human lung is approximately  $102 \text{ m}^2$  and assuming a 30% deposition fraction,<sup>(31,32)</sup> this would result in deposition of approximately  $0.3 \text{ mg/m}^2$  in the lung. Importantly, however, human exposure can be much higher. For example, in two epidemiological studies, one study determined that workers were exposed to levels of MWCNT up to  $6.11 \text{ µg/m}^3$  and the other study determined that workers were exposed to levels of CNT up to  $42.6 \text{ µg/m}^3$ .<sup>(33)</sup> In addition, recommended exposure levels for different CNT vary widely between countries, from 1 to  $50 \text{ µg/m}^3$ .<sup>(34)</sup> Thus, administration of 1 mg MWCNT/rat is a

reasonable dose for initial investigations into the carcinogenicity of an inhaled MWCNT.

While not the main theme of the present study, our collective results suggest that TIPS can be used to identify agents that are potentially carcinogenic to the lung and pleural mesothelium. Previously, we reported that male rats were each administered a total of  $1.25 \text{ mg}$  MWCNT (MWCNT-M or MWCNT-N) over a 9-day period using TIPS. The rats were killed 6 h after the final administration. Hyperplastic visceral mesothelial proliferation was clearly observed in the MWCNT-treated groups.<sup>(11)</sup> These results coupled with the results of the present study suggest the possibility that proliferative lesions seen shortly after administration of MWCNT in the previous study could transform into preneoplastic lesions and, ultimately, into the neoplastic lesions observed in the present study. Thus, TIPS, which can be used by numerous research groups, can be employed as a preliminary screening method for hazard identification of respirable materials. Given the increasing production and wide use of nanomaterials, it is a practical impossibility to evaluate their risk using standard whole body inhalation testing, especially considering the low number of research groups that have access to such testing systems. Therefore, it is essential that less expensive, widely available screening methods for hazard identification of nanoparticles (and other respirable materials) are developed to lessen the number of materials that need to be assessed by 2-year whole body inhalation assays to manageable levels.

The route of translocation of MWCNT from the lung to the pleura remains to be established. Penetration of MWCNT

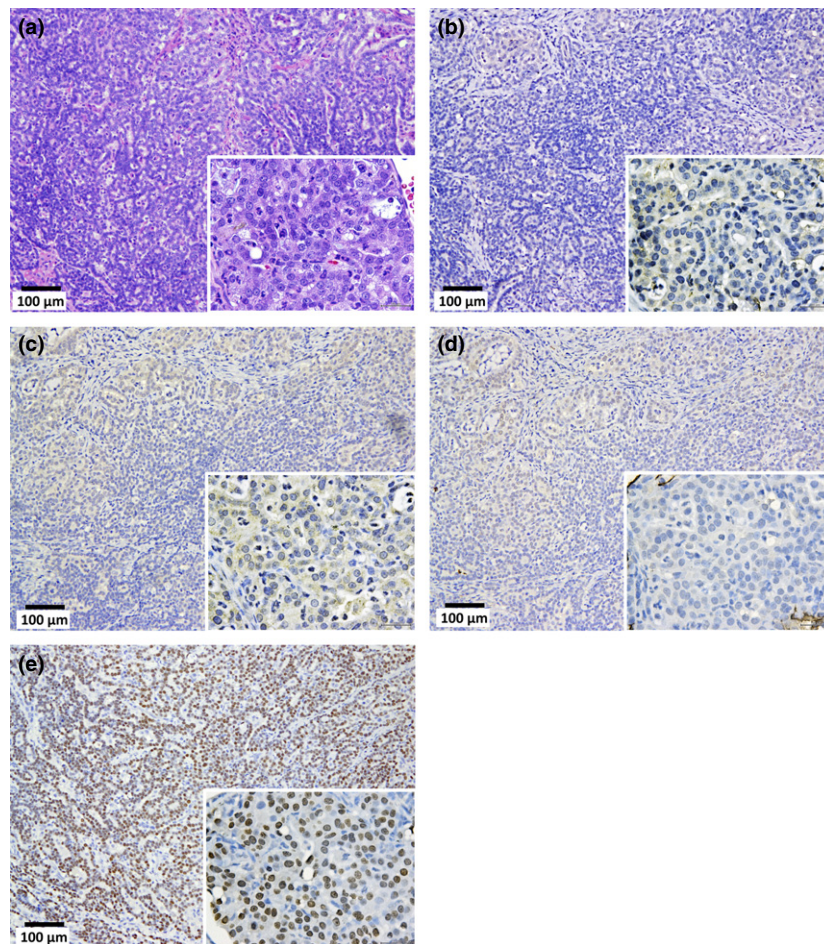


**Fig. 11.** Adenocarcinoma of the lung forming a large mass in the pleural cavity with invasion of the peribronchial lymphnodes, serosal pericardium and diaphragm (see Fig. 3). Densely proliferating small tumor cells with round nuclei are arranged in an incomplete glandular or solid manner. H&E (a), calretinin (b), Wilms tumor protein (WT-1) (c), podoplanin (d) and thyroid transcription factor-1 (TTF-1) (e) staining. The cytoplasm is slightly stained by WT-1. All the nuclei are clearly positive for TTF-1 indicating lung alveolar cell origin. After histological examination, this case was initially diagnosed as an epithelial mesothelioma; however, after staining with TTF-1, the tumor was re-diagnosed as a lung adenocarcinoma.

**Table 4.** Tumor incidence in other organs†

MWCNT fraction	Rats	Abdominal cavity mesothelioma (%)	Leydig cell tumor (%)	Leukemia/lymphoma (%)	Subcutaneous fibroma (%)	Pureputial gland tumor (%)	Pituitary gland tumor (%)
NT	15	0	10 (66.7)	0	4 (26.7)	0	0
V	13	2 (15.4)	10 (76.9)	2 (15.4)	2 (15.4)	1 (7.7)	1 (7.7)
NT + V	28	2 (7.1)	20 (71.4)	2 (7.1)	2 (7.1)	1 (3.6)	1 (3.6)
U	13	1 (7.7)	9 (69.2)	4 (30.8)	0	0	1 (7.7)
FT	13	1 (7.7)	8 (61.5)	3 (23.1)	1 (7.7)	1 (7.7)	2 (15.4)
R	15	0	8 (53.3)	3 (20.0)	1 (6.7)	0	1 (6.7)
U + FT + R	41	2 (4.9)	25 (61.0)	10 (24.4)	2 (4.9)	1 (2.4)	4 (9.8)

Average length: U =  $4.2 \pm 2.9 \mu\text{m}$ ; FT =  $2.6 \pm 1.6 \mu\text{m}$ ; R was not measurable. †Including 1 adrenal cortical adenoma in NT, 1 liver adenoma in FT and 1 sarcoma of unknown origin in R. FT, flow-through; MWCNT, multiwalled carbon nanotubes; NT, no treatment; R, retained; U, unfiltered; V, vehicle.

through the visceral pleura in mice has been reported.<sup>(9,12,17)</sup> In contrast, accumulation of MWCNT in the mediastinal lymphnodes points to the possible involvement of lymphatic vessels in their translocation.<sup>(11,14,16,35,36)</sup> We demonstrated the presence of MWCNT in pleural lavage fluid collected shortly after its administration to the lung,<sup>(11,16)</sup> supporting the premise that MWCNT may be transported through the lymphatic systems. Clearly, future studies designed to elucidate the translocation route of MWCNT to the pleura are warranted.

To investigate size dependency of MWCNT on the induction of lung and mesothelial lesions, MWCNT-N was sieved to produce three preparations with different average lengths: unfiltered MWCNT-N ( $4.2 \pm 2.9 \mu\text{m}$ ), MWCNT-N in the

flow-through fraction ( $2.6 \pm 1.6 \mu\text{m}$ ), and the MWCNT retained by the sieve (not measurable due to the dense agglomerates the retained fibers formed due to the loss of the PF68 dispersant during filtration) (Table 1). Interestingly, in the rats administered unfiltered MWCNT-N, the size of the fibers in the lung tissue slides tended to be smaller than in the administered preparation (Table 1). The reason for the difference in the average size of the administered MWCNT and the MWCNT found in the lung is unknown; however, one possibility is that the longer MWCNT did not penetrate to the alveoli as efficiently as shorter MWCNT.

We did not observe any statistically significant differences in the incidence of mesothelial or bronchiolo-alveolar tumors

**Table 5. Physical characteristics of MWCNT-7 and MWCNT-N**

	MWCNT-7	MWCNT-N
Length	1–4 μm (38%)	1–4 μm (51%)
Length	5–20 μm (58%)	5–20 μm (47%)
Diameter	20–100 nm (98%)	30–100 nm (95%)
Layers	35–40	Unknown
Iron content	0.3–0.4%	0.04–0.05%

MWCNT, multiwalled carbon nanotubes.

induced by the different MWCNT-N preparations. However, it is noteworthy that both the unfiltered and flow-through fractions induced mesothelioma while the retained fraction did not. In addition, the incidence of lung tumors was higher (not statistically significant) in the rats administered the retained fraction of MWCNT. Although the reasons for these observations are not clear, it is possibly due to the formation of aggregates and agglomerates that impeded the movement/clearance of the MWCNT in the retained fraction.

Persistence of fibers in the lung and pleura is thought to be a key element in the toxic effects that fibers can have on these tissues.<sup>(3,37,38)</sup> In our study, the amount of MWCNT in the lung at week 109 was 25.4% (unfiltered MWCNT-N), 48.0% (flow-through fraction) and 26.3% (retained fraction) of the amount of MWCNT in the lung 24 h after the last administration of MWCNT at week 2. This is comparable to the amount of MWCNT retained in the mouse lung 48 weeks after exposure to MWCNT.<sup>(25)</sup> In that study, the total lung burden of MWCNT 1 and 336 days after inhalation exposure to MWCNT was  $28.1 \pm 0.8 \mu\text{g}$  and  $18.3 \pm 1.1 \mu\text{g}$ , respectively; assuming linear clearance of MWCNT from the lung, the lung burden at 109 weeks would be approximately  $6 \mu\text{g}$  or 21% of the burden at day 1 post-exposure. Therefore, induction of malignant mesothelioma and lung alveolar cell tumors in the present study was unlikely to be due to abnormal clearance of MWCNT from the lung.

Tumors developed in the areas of MWCNT deposition, the lung and mediastinal space. The main deposition site in the lung tissue at the time of death was in alveolar macrophages and small alveolar–granulomatous lesions. Deposition was also observed in the mediastinal and bronchial lymph nodes and the periphery of the tumor tissues, both lung tumors and malignant mesotheliomas. As noted above, our previous studies showed that administration of MWCNT to the lung caused an inflammatory response, and this response could be relevant to MWCNT-induced cancer development.<sup>(39–42)</sup> In addition, generation of cytotoxic oxygen radicals and cytokines by activated macrophages might be involved in the generation and growth

of tumor cells.<sup>(11,16,43–45)</sup> Observations in our previous study that mesothelial cell proliferation is enhanced by conditioned macrophage culture media and by the supernatants of pleural cavity lavage are consistent with this premise.<sup>(11)</sup>

Iron impurities in MWCNT may possibly play a role in MWCNT toxicity.<sup>(46)</sup> However, iron containing MWCNT does not appear to generate radicals *in vivo*.<sup>(47)</sup> In the present study, MWCNT with an iron content of only 0.046% by weight, approximately 10-fold lower than the iron content of the MWCNT used by Aldieri *et al.* (0.420%)<sup>(46)</sup> or Fenoglio *et al.* (0.47%),<sup>(47)</sup> was carcinogenic to both the lung and pleura, suggesting that the iron content of MWCNT may not be of primary importance in MWCNT-mediated carcinogenicity. In contrast, an alternative hypothesis for a role of iron in MWCNT-induced cell injury and carcinogenesis has been proposed by Wang *et al.*<sup>(48)</sup> These authors report that hemoglobin and transferrin can adsorb onto the surface of MWCNT, and that the MWCNT–hemoglobin–transferrin complex can bind to transferrin receptor 1 and be endocytosed into rat peritoneal mesothelial cells *in vitro*. This resulted in iron overload in the cell and subsequent DNA damage. Thus, even iron-free MWCNT could transport excess iron into a cell, resulting in iron-mediated DNA damage. The role of iron in mesothelioma induction *in vivo* clearly warrants further investigation.

In conclusion, exposure of rats to 1 mg MWCNT-N per rat via the airway, the exposure route that is relevant to humans, results in malignant mesothelioma and lung alveolar cell tumors. This is the first report to document the induction of lung and mesothelial tumors in rats administered MWCNT via the airway and extends the IARC classification of MWCNT-7 as a group 2B carcinogen to other species of MWCNT.

### Acknowledgments

We wish to thank Dr Vincent Castranova for his valuable comments and advice. This work was supported by Health and Labor Sciences Research Grants of Japan (H21-kagaku-ippan-008, H22-kagaku-ippan-005, H25-kagaku-ippan-004, H24-kagaku-sitei-009) and by the Princess Takamatsu Cancer Research Fund (H24).

### Disclosure Statement

The authors have no conflicts of interest to declare.

### Disclaimer

The findings and conclusions in this report are those of the authors and do not necessarily represent the views of the Ministry of Health, Labour and Welfare, Japan.

### References

- Donaldson K, Poland CA. Nanotoxicology: new insights into nanotubes. *Nat Nanotechnol* 2009; **4**: 708–10.
- Kohyama N, Suzuki Y. Analysis of asbestos fibers in lung parenchyma, pleural plaques, and mesothelioma tissues of North American insulation workers. *Ann N Y Acad Sci* 1991; **643**: 27–52.
- Donaldson K, Poland CA, Murphy FA, MacFarlane M, Chernova T, Schinwald A. Pulmonary toxicity of carbon nanotubes and asbestos – Similarities and differences. *Adv Drug Deliv Rev* 2013; **65**: 2078–86.
- Takagi A, Hirose A, Nishimura T *et al.* Induction of mesothelioma in p53 +/– mouse by intraperitoneal application of multi-wall carbon nanotube. *J Toxicol Sci* 2008; **33**: 105–16.
- Sakamoto Y, Nakae D, Fukumori N *et al.* Induction of mesothelioma by a single intrascrotal administration of multi-wall carbon nanotube in intact male Fischer 344 rats. *J Toxicol Sci* 2009; **34**: 65–76.

- Nagai H, Okazaki Y, Chew SH *et al.* Diameter and rigidity of multiwalled carbon nanotubes are critical factors in mesothelial injury and carcinogenesis. *Proc Natl Acad Sci USA* 2011; **108**: E1330–8.
- Takagi A, Hirose A, Futakuchi M, Tsuda H, Kanno J. Dose-dependent mesothelioma induction by intraperitoneal administration of multi-wall carbon nanotubes in p53 heterozygous mice. *Cancer Sci* 2012; **103**: 1440–4.
- Donaldson K, Murphy FA, Duffin R, Poland CA. Asbestos, carbon nanotubes and the pleural mesothelium: a review of the hypothesis regarding the role of long fibre retention in the parietal pleura, inflammation and mesothelioma. *Part Fibre Toxicol* 2010; **7**: 5.
- Mercer RR, Hubbs AF, Scabilloni JF *et al.* Distribution and persistence of pleural penetrations by multi-walled carbon nanotubes. *Part Fibre Toxicol* 2010; **7**: 28.
- Porter DW, Hubbs AF, Mercer RR *et al.* Mouse pulmonary dose- and time course-responses induced by exposure to multi-walled carbon nanotubes. *Toxicology* 2010; **269**: 136–47.

- 11 Xu J, Futakuchi M, Shimizu H *et al.* Multi-walled carbon nanotubes translocate into the pleural cavity and induce visceral mesothelial proliferation in rats. *Cancer Sci* 2012; **103**: 2045–50.
- 12 Mercer RR, Scabilloni JF, Hubbs AF *et al.* Extrapulmonary transport of MWCNT following inhalation exposure. *Part Fibre Toxicol* 2013; **10**: 38.
- 13 Murphy FA, Poland CA, Duffin R, Donaldson K. Length-dependent pleural inflammation and parietal pleural responses after deposition of carbon nanotubes in the pulmonary airspaces of mice. *Nanotoxicology* 2013; **7**: 1157–67.
- 14 Porter DW, Hubbs AF, Chen BT *et al.* Acute pulmonary dose-responses to inhaled multi-walled carbon nanotubes. *Nanotoxicology* 2013; **7**: 1179–94.
- 15 Kasai T, Umeda Y, Ohnishi M *et al.* Thirteen-week study of toxicity of fiber-like multi-walled carbon nanotubes with whole-body inhalation exposure in rats. *Nanotoxicology* 2014; **9**: 1–10.
- 16 Xu J, Alexander DB, Futakuchi M *et al.* Size- and shape-dependent pleural translocation, deposition, fibrogenesis, and mesothelial proliferation by multi-walled carbon nanotubes. *Cancer Sci* 2014; **105**: 763–9.
- 17 Ryman-Rasmussen JP, Cesta MF, Brody AR *et al.* Inhaled carbon nanotubes reach the subpleural tissue in mice. *Nat Nanotechnol* 2009; **4**: 747–51.
- 18 Li ZF, Luo GH, Wei F, Xiang R, Liu YP. The quantitative characterization of the concentration and dispersion of multi-walled carbon nanotubes in suspension by spectrophotometry. *Nanotechnology* 2006; **17**: 3692–8.
- 19 Xu J, Futakuchi M, Iigo M *et al.* Involvement of macrophage inflammatory protein 1 $\alpha$  (MIP1 $\alpha$ ) in promotion of rat lung and mammary carcinogenic activity of nanoscale titanium dioxide particles administered by intrapulmonary spraying. *Carcinogenesis* 2010; **31**: 927–35.
- 20 Xu J, Futakuchi M, Alexander DB *et al.* Nanosized zinc oxide particles do not promote DHPN-induced lung carcinogenesis but cause reversible epithelial hyperplasia of terminal bronchioles. *Arch Toxicol* 2014; **88**: 65–75.
- 21 Numano T, Xu J, Futakuchi M *et al.* Comparative study of toxic effects of anatase and rutile type nanosized titanium dioxide particles *in vivo* and *in vitro*. *Asian Pac J Cancer Prev* 2014; **15**: 929–35.
- 22 Ohnishi M, Yajima H, Kasai T *et al.* Novel method using hybrid markers: development of an approach for pulmonary measurement of multi-walled carbon nanotubes. *J Occup Med Toxicol* 2013; **8**: 30.
- 23 Blackshear PE, Pandiri AR, Ton TV *et al.* Spontaneous mesotheliomas in F344/N rats are characterized by dysregulation of cellular growth and immune function pathways. *Toxicol Pathol* 2014; **42**: 863–76.
- 24 Ma-Hock L, Treumann S, Strauss V *et al.* Inhalation toxicity of multiwall carbon nanotubes in rats exposed for 3 months. *Toxicol Sci* 2009; **112**: 468–81.
- 25 Mercer RR, Scabilloni JF, Hubbs AF *et al.* Distribution and fibrotic response following inhalation exposure to multi-walled carbon nanotubes. *Part Fibre Toxicol* 2013; **10**: 33.
- 26 Pauluhn J. Subchronic 13-week inhalation exposure of rats to multiwalled carbon nanotubes: toxic effects are determined by density of agglomerate structures, not fibrillar structures. *Toxicol Sci* 2010; **113**: 226–42.
- 27 Yu KN, Kim JE, Seo HW, Chae C, Cho MH. Differential toxic responses between pristine and functionalized multiwall nanotubes involve induction of autophagy accumulation in murine lung. *J Toxicol Environ Health A* 2013; **76**: 1282–92.
- 28 Sargent LM, Porter DW, Staska LM *et al.* Promotion of lung adenocarcinoma following inhalation exposure to multi-walled carbon nanotubes. *Part Fibre Toxicol* 2014; **11**: 3.
- 29 Stone KC, Mercer RR, Gehr P, Stockstill B, Crapo JD. Allometric relationships of cell numbers and size in the mammalian lung. *Am J Respir Cell Mol Biol* 1992; **6**: 235–43.
- 30 Galer DM, Leung HW, Sussman RG, Trzos RJ. Scientific and practical considerations for the development of occupational exposure limits (OELs) for chemical substances. *Regul Toxicol Pharmacol* 1992; **15**: 291–306.
- 31 Bates DV, Fish BR, Hatch TF, Mercer TT, Morrow PE. Deposition and retention models for internal dosimetry of the human respiratory tract. Task group on lung dynamics. *Health Phys* 1966; **12**: 173–207.
- 32 Environmental Protection Agency. Air Quality Criteria for Particulate Matter, Vol. II. 2004; Environmental Protection Agency. Washington DC. Document EPA/600/P-99/002bF.
- 33 Liou SH, Tsai CS, Pelclova D, Schubauer-Berigan MK, Schulte PA. Assessing the first wave of epidemiological studies of nanomaterial workers. *J Nanopart Res* 2015; **17**: 413.
- 34 Fatkhutdinova LM, Khaliullin TO, Shvedova AA. Carbon nanotubes exposure risk assessment: From toxicology to epidemiologic studies (overview of the current problem). *Nanotechnol Russ* 2015; **10**: 501–9.
- 35 Aiso S, Kubota H, Umeda Y *et al.* Translocation of intratracheally instilled multiwall carbon nanotubes to lung-associated lymph nodes in rats. *Ind Health* 2011; **49**: 215–20.
- 36 Sargent LM, Reynolds SH, Castranova V. Potential pulmonary effects of engineered carbon nanotubes: *in vitro* genotoxic effects. *Nanotoxicology* 2010; **4**: 396–408.
- 37 Murphy FA, Poland CA, Duffin R *et al.* Length-dependent retention of carbon nanotubes in the pleural space of mice initiates sustained inflammation and progressive fibrosis on the parietal pleura. *Am J Pathol* 2011; **178**: 2587–600.
- 38 Costa R, Orriols R. Man-made mineral fibers and the respiratory tract. *Arch Bronconeumol* 2012; **48**: 460–8.
- 39 Colotta F, Allavena P, Sica A, Garlanda C, Mantovani A. Cancer-related inflammation, the seventh hallmark of cancer: links to genetic instability. *Carcinogenesis* 2009; **30**: 1073–81.
- 40 Coussens LM, Werb Z. Inflammation and cancer. *Nature* 2002; **420**: 860–7.
- 41 Cruz SM, Balkwill FR. Inflammation and cancer: advances and new agents. *Nat Rev Clin Oncol* 2015; **12**: 584–96.
- 42 Lu H, Ouyang W, Huang C. Inflammation, a key event in cancer development. *Mol Cancer Res* 2006; **4**: 221–33.
- 43 Barna BP, Huizar I, Malur A *et al.* Carbon nanotube-induced pulmonary granulomatous disease: Twist1 and alveolar macrophage M1 activation. *Int J Mol Sci* 2013; **14**: 23858–71.
- 44 Meng J, Li X, Wang C, Guo H, Liu J, Xu H. Carbon nanotubes activate macrophages into a M1/M2 mixed status: recruiting naive macrophages and supporting angiogenesis. *ACS Appl Mater Interfaces* 2015; **7**: 3180–8.
- 45 Murphy FA, Schinwald A, Poland CA, Donaldson K. The mechanism of pleural inflammation by long carbon nanotubes: interaction of long fibres with macrophages stimulates them to amplify pro-inflammatory responses in mesothelial cells. *Part Fibre Toxicol* 2012; **9**: 8.
- 46 Aldieri E, Fenoglio I, Cesano F *et al.* The role of iron impurities in the toxic effects exerted by short multiwalled carbon nanotubes (MWCNT) in murine alveolar macrophages. *J Toxicol Environ Health* 2013; **76**: 1056–71.
- 47 Fenoglio I, Tomatis M, Lison D *et al.* Reactivity of carbon nanotubes: free radical generation or scavenging activity? *Free Radic Biol Med* 2006; **40**: 1227–33.
- 48 Wang Y, Okazaki Y, Shi L *et al.* Role of hemoglobin and transferrin in multi-wall carbon nanotube-induced mesothelial injury and carcinogenesis. *Cancer Sci* 2016; **107**: 250–7.